

# Emplacement dynamics of syn-collapse ring dikes: an example from the Altenberg–Teplice caldera, Bohemian Massif

Filip Tomek<sup>1,2\*</sup>, Jiří Žák<sup>1</sup>, Martin Svojtka<sup>1</sup>, Fritz Finger<sup>3</sup> and Michael Waitzinger<sup>3</sup>

<sup>1</sup>Czech Academy of Sciences, Institute of Geology, Rozvojová 269, Prague, 16500, Czech Republic

<sup>2</sup> Institute of Geology and Paleontology, Faculty of Science, Charles University, Albertov 6, Prague, 12843, Czech Republic

<sup>3</sup> Department of Chemistry and Physics of Materials, University of Salzburg, Jakob Haringer Strasse 2A, A-5020, Salzburg, Austria

\*corresponding author e-mail: [filip.tomek@gmail.com](mailto:filiptomek@gmail.com)

---

## Data Repository

### Items

1.	Geochemical data (porphyritic microgranite, Teplice rhyolite).....	2
2.	Laser ablation inductively coupled plasma mass spectrometry (LA-ICP-MS) – methods .....	4
3.	U-Th-Pb isotopic data (porphyritic microgranite).....	7
4.	Cathodoluminescence images of selected zircon grains (porphyritic microgranite).....	11
5.	Anisotropy of magnetic susceptibility (AMS) - methods.....	12
6.	Anisotropy of magnetic susceptibility (AMS) – data.....	16
7.	Anisotropy of magnetic susceptibility (AMS) – maps of $k_m$ and $P$ parameters.....	18
8.	Frequency–susceptibility dependence .....	19
9.	Apparent width of dikes vs. various AMS parameters.....	20

## Data Repository Item 1

Ref	Sample No	SiO <sub>2</sub>	Al <sub>2</sub> O <sub>3</sub>	Fe <sub>2</sub> O <sub>3</sub>	FeO	Fe <sub>2</sub> O <sub>3t</sub>	MnO	MgO	CaO	Na <sub>2</sub> O	K <sub>2</sub> O	TiO <sub>2</sub>	P <sub>2</sub> O <sub>5</sub>	H <sub>2</sub> O+	H <sub>2</sub> O-	CO <sub>2</sub>	Total	Cr	Pb	Zn	Sn	Rb	Cs	Sr	Ga	Li	Nb	Hf	Zr	Y	Th	U	La	Ce	Pr	Nd	Sm	Gd	Dy
	K1349	71.86	13.4	1.2	1.4	n.a.	0.1	0.3	1.0	3.3	5.8	0.3	0.1	0.6	0.1	0.0	99.6	25	110	38	1	206	n.a.	112	20	27	14	n.a.	253	38	32	10	n.a.						
11	K1351	70.74	13.9	1.0	1.8	n.a.	0.1	0.5	1.1	3.3	5.8	0.3	0.1	0.8	0.1	0.0	99.6	15	100	58	1	202	n.a.	111	19	27	10	n.a.	280	38	28	9	n.a.						
	K1355	72.51	13.1	0.9	1.2	n.a.	0.0	0.3	0.6	3.6	6.0	0.3	0.1	0.8	0.1	0.0	99.6	12	66	79	1	238	n.a.	72	10	42	13	n.a.	232	36	36	9	n.a.						
	3210	75.82	12.2	0.4	0.4	n.a.	0.1	0.0	0.8	5.0	0.0	0.1	0.0	0.3	n.a.	n.a.	99.1	n.a.	n.a.	n.a.	11	399	8	26	20	n.a.	17	5	93	45	60	16	33	79	10	40	10	8	8
12	3208	76.35	11.8	1.0	0.4	n.a.	0.1	0.0	0.5	6.3	0.0	0.1	0.0	0.3	n.a.	n.a.	96.9	n.a.	n.a.	n.a.	3	248	11	22	17	n.a.	10	5	149	22	28	6	55	116	13	47	7	5	4
	3207	77.07	11.6	0.3	0.2	n.a.	0.1	0.0	1.1	4.7	0.0	0.1	n.a.	n.a.	n.a.	n.a.	95.2	n.a.	n.a.	n.a.	13	394	10	11	21	n.a.	22	6	97	67	44	29	20	52	7	29	9	10	12
	3194	76.11	12.7	1.1	0.2	n.a.	0.1	0.0	0.6	5.1	0.0	0.1	n.a.	n.a.	n.a.	n.a.	96.1	n.a.	n.a.	n.a.	6	393	17	25	22	n.a.	20	7	146	60	62	17	47	104	12	44	9	9	10
Teplice rhyolite	3201	76.43	12.3	1.2	0.2	n.a.	0.0	0.1	0.1	1.8	5.4	0.1	0.0	n.a.	1.5	0.0	99.9	n.a.	n.a.	n.a.	4	246	21	27	17	n.a.	14	5	150	36	32	7	49	110	12	46	8	7	7
	3198	75.47	12.3	1.3	0.3	n.a.	0.0	0.2	0.6	2.1	5.6	0.1	0.0	n.a.	1.5	0.4	99.9	n.a.	n.a.	n.a.	86	475	20	16	21	n.a.	58	7	123	76	59	13	38	91	11	42	10	11	13
14	TU	78.20	11.8	0.7	0.4	n.a.	0.0	0.1	0.3	1.7	4.8	0.1	0.0	n.a.	n.a.	n.a.	98.1	n.a.	n.a.	n.a.	230	n.a.	16	n.a.	n.a.	n.a.	n.a.	140	n.a.										
	TPR1a	78.50	11.5	0.5	0.2	n.a.	0.0	0.1	0.4	3.2	4.5	0.1	0.0	n.a.	n.a.	n.a.	99.0	n.a.	n.a.	n.a.	330	n.a.	17	n.a.	n.a.	n.a.	n.a.	95	n.a.										
	TPR1b	77.50	12.0	1.1	0.3	n.a.	0.0	0.1	0.4	2.5	5.5	0.1	0.0	n.a.	n.a.	n.a.	99.5	n.a.	n.a.	n.a.	265	n.a.	30	n.a.	n.a.	n.a.	n.a.	145	n.a.										
15	TR3a	75.90	12.3	0.9	0.7	1.7	0.3	0.1	0.6	3.3	5.2	0.1	0.0	n.a.	n.a.	n.a.	101.1	n.a.	n.a.	n.a.	296	n.a.	49	n.a.	n.a.	n.a.	n.a.	168	n.a.										
	TR3b	75.60	12.2	0.9	0.6	1.6	0.0	0.1	0.6	3.0	5.6	0.2	0.1	n.a.	n.a.	n.a.	100.4	n.a.	n.a.	n.a.	285	n.a.	48	n.a.	n.a.	n.a.	n.a.	152	n.a.										
	TR3c	72.10	13.4	0.9	1.4	2.5	0.1	0.3	0.7	3.3	5.9	0.3	0.1	n.a.	n.a.	n.a.	101.0	n.a.	n.a.	n.a.	229	n.a.	84	n.a.	n.a.	n.a.	n.a.	244	n.a.										
16	TR1a	80.90	11.8	n.a.	n.a.	1.0	n.a.	0.2	0.1	0.1	3.0	0.0	0.0	n.a.	n.a.	n.a.	97.1	n.a.	17	60	52	279	17	13	18	n.a.	18	3	63	65	31	8	38	103	14	57	16	12	11
	TR1b	78.30	12.9	n.a.	n.a.	2.3	n.a.	0.3	0.1	0.1	3.4	0.1	0.0	n.a.	n.a.	n.a.	97.5	n.a.	7	43	37	247	9	4	21	n.a.	22	4	90	26	34	6	8	23	3	9	3	3	4
	TR2a	77.40	12.5	n.a.	n.a.	2.3	n.a.	0.2	0.1	0.2	5.0	0.1	0.0	n.a.	n.a.	n.a.	97.7	n.a.	11	74	14	307	10	76	22	n.a.	20	6	153	39	43	7	37	63	8	26	5	5	6
	TR2b	77.50	12.6	1.1	0.3	1.5	0.0	0.1	0.3	1.4	5.7	0.1	0.0	n.a.	n.a.	n.a.	100.7	n.a.	32	26	74	487	20	36	18	n.a.	12	7	179	55	63	17	64	131	16	54	11	9	10
	TR3a	74.20	13.7	n.a.	n.a.	1.5	n.a.	0.2	0.9	2.3	5.8	0.2	0.0	n.a.	n.a.	n.a.	98.9	n.a.	34	55	9	566	30	55	15	n.a.	11	7	209	41	38	9	72	140	16	53	10	8	8
	TR/RD	73.70	13.8	n.a.	n.a.	3.0	n.a.	0.1	0.1	0.8	7.0	0.2	0.0	n.a.	n.a.	n.a.	98.7	n.a.	34	94	12	473	21	32	24	n.a.	13	6	203	29	32	6	31	77	7	23	5	4	5

Note: n.a. - not analyzed or not given by the authors; n.d. - not detected; References: 1 - this study; 2 and 10 - Štemprok et al. 2003; 3 and 11 - Schovánek 2001a; 4 - Jiránek 1989b; 5 - Muller and Seltmann 2002; 6 - Breiter et al. 2001 and Breiter 1996; 7 and 12 - Breiter 2012 and Breiter and Škoda 2017; 8 and 16 - Seltmann and Breiter 1985; 9 - Hrouda et al. 2002; 13 - Breiter et al. 2012; 14 - Breiter 1996; 15 - Breiter et al. 2001

## Data Repository Item 2

### U–Pb ZIRCON GEOCHRONOLOGY USING LASER ABLATION ICP-MS

#### Method

Zircon grains were separated from the 10–15 kg of fresh rock sample using conventional separation techniques. After separation, individual morphological types of zircons were arranged along their c-axis and mounted in one-inch epoxy disc that was grind and finally polished. Internal zircon structure in individual zircon growth zones was checked by cathodoluminescence (CL) imaging using a JEOL JXA-8530F electron probe microanalyzer at the Faculty of Science, Charles University. An Element 2 high-resolution double focusing magnetic sector field ICP–MS (Thermo Scientific) coupled with a 213-nm NdYAG UP-213 laser ablation system (New Wave Research) at the Czech Academy of Sciences, Institute of Geology was used to acquire the Pb/U isotopic ratios. Samples were ablated in an in-house small volume ablation cell, construction inspired by a conception of Kooijman et al. (2012). The laser was fired at a repetition rate of 5 Hz, using a spot size of 30  $\mu\text{m}$  and a fluence of c. 4–5  $\text{J}/\text{cm}^2$ . Acquisitions for all measured samples consisted of a 30 s measurement of blank followed by U and Pb signals from zircons for another 30 s interval. Data were collected for masses 204, 206, 207, 208, 232 and 238 using both analogue and ion counting modes of the SEM detector, one point per mass peak and relevant dwell times per mass of 10, 15, 30, 10, 10 and 15 ms. The Hg impurity in the carrier He gas, which can cause isobaric interference of  $^{204}\text{Hg}$  on  $^{204}\text{Pb}$  and the relative contribution of common Pb to total Pb, were reduced by in-house made gold-coated sand trap. The relative contribution of common Pb to total Pb was less than 0.1 % and, therefore, no common Pb correction was applied to the data. Elemental fractionation and instrumental mass bias were corrected by normalization of internal U–Pb calibration zircon standard 91500 (1065 Ma, Wiedenbeck et al., 1995), and reference natural zircon standards GJ-1 (609 Ma, Jackson et al., 2004; 603 Ma, Kylander-

Clark et al., 2013), and Plešovice (337 Ma, Sláma et al., 2008), periodically analyzed during the measurement for quality control purposes. Raw data reduction, age calculations, including corrections for baseline, instrumental drift, mass bias and down-hole fractionation, and graphical presentation of concordia diagrams were generated with Iolite program (Paton et al., 2011). Standard error ages are quoted at 2 sigma absolute followed calculations recommended by Horstwood et al. (2016).

## REFERENCES

- Horstwood, M.S.A., Košler, J., Gehrels, G., Jackson, S.E., McLean, N.M., Paton, C., Pearson, N.J., Sircombe, K., Sylvester, P., Vermeesch, P., Bowring, J.F., Condon, D.J., Schoene, B., 2016. Community-Derived Standards for LA-ICP-MS U-(Th-)Pb Geochronology – Uncertainty Propagation, Age Interpretation and Data Reporting. *Geostandards and Geoanalytical Research* 40, 311–332.
- Jackson, S.E., Pearson, N.J., Griffin, W.L., Belousova, E.A., 2004. The application of laser ablation-inductively coupled plasma-mass spectrometry to in situ U-Pb zircon geochronology. *Chemical Geology* 211, 47–69.
- Kooijman, E., Berndt, J., Mezger, K., 2012. U-Pb dating of zircon by laser ablation ICP-MS: recent improvements and new insights. *European Journal of Mineralogy* 24, 5–21.
- Kylander-Clark, A.R.C., Hacker, B.R., Cottle, J.M., 2013. Laser-ablation split-stream ICP petrochronology. *Chemical Geology* 345, 99–112.
- Paton, C., Hellstrom, J., Paul, B., Hergt, J., 2011. Iolite : Freeware for the visualisation and processing of mass spectrometric 2508–2518.
- Sláma, J., Košler, J., Condon, D.J., Crowley, J.L., Gerdes, A., Hanchar, J.M., Horstwood, M.S.A., Morris, G.A., Nasdala, L., Norberg, N., Schaltegger, U., Schoene, B., Tubrett, M.N., Whitehouse, M.J., 2008. Plešovice zircon - A new natural reference material for U-Pb and Hf isotopic microanalysis. *Chemical Geology* 249, 1–35.

Wiedenbeck, M., Allé, P., Corfu, F., Griffin, W.L.W., Meier, M., Oberli, F., von Quadt, A.,  
Roddick, J.C., Spiegel, W., 1995. Three Natural Zircon Standards for U-Th-Pb, Lu-Hf,  
Trace Element and Ree Analyses. *Geostandards and Geoanalytical Research* 19, 1–23.

### Data Repository Item 3

**Laser ablation ICP-MS U-Pb zircon data (sample FT13)**

Analysis	Corrected isotope ratios					Apparent ages (Ma)					U, Th and Pb content (ppm)					Th/U
	$^{207}\text{Pb}/^{235}\text{U}$	$\pm 2\sigma$	$^{206}\text{Pb}/^{238}\text{U}$	$\pm 2\sigma$	error corr.	$^{207}\text{Pb}/^{235}\text{U}$	$\pm 2\sigma$	$^{206}\text{Pb}/^{238}\text{U}$	$\pm 2\sigma$	Approx U	$\pm 2\sigma$	Approx Th	$\pm 2\sigma$	Approx Pb	$\pm 2\sigma$	
1	0.3686	0.0086	0.0502	0.0005	0.3584	318	6	316	3	146	2.6	71	1.6	11	0.28	0.5
2	0.3672	0.0082	0.0499	0.0005	0.2454	317	6	314	3	151	2.3	59	0.77	9	0.17	0.4
3	0.3594	0.0070	0.0485	0.0005	0.5366	312	5	305	3	451	6.6	181	1.8	28	0.34	0.4
4	0.3697	0.0082	0.0499	0.0005	0.0151	319	6	314	3	216	4.6	120	2.8	18	0.44	0.6
5	0.3622	0.0075	0.0494	0.0006	0.4959	314	6	311	4	277	8.0	151	3.7	23	0.6	0.5
6	0.3714	0.0075	0.0502	0.0006	0.2592	321	6	315	3	287	4.9	113	1.6	18	0.32	0.4
7	0.3737	0.0089	0.0505	0.0005	0.1137	323	6	318	3	141	1.5	64	0.52	10	0.18	0.5
8	0.3633	0.0091	0.0490	0.0006	0.1689	315	7	309	4	119	0.9	72	0.74	11	0.24	0.6
9	0.3680	0.0097	0.0497	0.0006	0.3208	317	7	312	4	95	2.5	49	1.3	7	0.22	0.5
10	0.3650	0.0098	0.0494	0.0006	0.2241	315	7	311	3	87	1.7	51	0.9	8	0.16	0.6
11	0.3602	0.0083	0.0494	0.0005	0.2471	312	6	311	3	114	1.7	68	0.91	10	0.18	0.6
12	0.3578	0.0077	0.0493	0.0005	0.2847	310	6	310	3	278	8.3	146	5.6	21	0.8	0.5
13	0.3619	0.0095	0.0487	0.0005	0.0775	313	7	306	3	99	1.4	70	0.81	10	0.2	0.7
14	0.3583	0.0078	0.0488	0.0005	0.3312	311	6	307	3	226	2.9	106	1.3	15	0.28	0.5
15	0.3669	0.0084	0.0497	0.0005	0.1078	317	6	313	3	171	3.3	96	2.2	14	0.37	0.6
16	0.3654	0.0081	0.0501	0.0005	0.3643	316	6	315	3	183	2.6	96	1.3	15	0.26	0.5
17	0.3584	0.0075	0.0494	0.0005	0.2011	310	6	311	3	211	4.8	132	4.3	20	0.7	0.6
18	0.3654	0.0073	0.0496	0.0005	0.3009	316	5	312	3	243	2.6	166	2.6	24	0.56	0.7
19	0.3576	0.0080	0.0495	0.0005	0.3731	310	6	312	3	196	3.1	86	1.2	13	0.25	0.4
20	0.3706	0.0080	0.0510	0.0006	0.5599	320	6	320	4	325	15.0	181	8.5	28	1.1	0.6
21	0.3538	0.0092	0.0494	0.0005	0.1206	307	7	311	3	155	2.1	99	1.4	15	0.28	0.6
22	0.3546	0.0098	0.0489	0.0006	0.1194	307	7	308	3	90	0.6	42	0.27	6	0.16	0.5
23	0.3615	0.0100	0.0500	0.0006	0.2575	314	8	315	4	116	3.1	62	2.3	9	0.37	0.5
24	0.3637	0.0078	0.0500	0.0005	0.1997	315	6	314	3	176	2.6	81	0.91	12	0.2	0.5
25	0.3657	0.0110	0.0490	0.0006	0.0732	316	8	308	4	80	0.7	41	0.84	6	0.18	0.5
26	0.3563	0.0085	0.0490	0.0005	0.0880	309	6	308	3	182	1.6	80	0.79	12	0.22	0.4
27	0.3566	0.0078	0.0488	0.0005	0.1849	309	6	308	3	222	7.4	100	2.9	15	0.39	0.4
28	0.3641	0.0076	0.0490	0.0004	0.2402	315	6	308	3	235	5.2	111	4.5	16	0.72	0.5
29	0.3602	0.0071	0.0490	0.0005	0.5554	312	5	309	3	412	5.8	179	1.9	27	0.34	0.4
30	0.3547	0.0100	0.0488	0.0006	0.2270	309	8	307	4	98	1.2	59	0.47	9	0.21	0.6
31	0.3651	0.0068	0.0495	0.0005	0.6109	316	5	311	3	737	13.0	202	1.8	32	0.4	0.3
32	0.3613	0.0095	0.0490	0.0005	0.2460	313	7	308	3	129	4.4	71	3.3	10	0.5	0.6
33	0.3655	0.0076	0.0498	0.0005	0.1845	316	6	313	3	218	3.8	88	1.1	13	0.24	0.4
34	0.3686	0.0075	0.0500	0.0004	0.3022	318	6	315	3	303	3.9	133	1.5	20	0.34	0.4
35	0.3456	0.0072	0.0483	0.0006	0.5831	301	5	304	4	466	7.3	395	8.7	59	1.4	0.8
36	0.3650	0.0100	0.0495	0.0005	0.1972	316	7	311	3	120	1.5	59	0.72	9	0.23	0.5
37	0.3600	0.0075	0.0496	0.0006	0.5144	312	6	312	4	385	7.0	225	3	35	0.54	0.6
38	0.3638	0.0079	0.0500	0.0005	0.2319	315	6	314	3	276	3.8	162	2.1	25	0.37	0.6
39	0.3599	0.0089	0.0499	0.0005	0.2757	312	7	314	3	179	4.8	109	4.6	17	0.7	0.6
40	0.3736	0.0094	0.0502	0.0005	0.0903	322	7	316	3	138	2.8	63	1.2	10	0.24	0.5
41	0.3652	0.0077	0.0504	0.0005	0.4339	316	6	317	3	239	3.1	89	0.92	14	0.23	0.4
42	0.3629	0.0087	0.0495	0.0005	0.1964	314	7	311	3	169	1.8	95	0.8	14	0.27	0.6
43	0.3592	0.0082	0.0498	0.0005	0.2949	312	6	313	3	236	4.1	90	1.2	13	0.24	0.4
44	0.3630	0.0079	0.0498	0.0005	0.2767	314	6	314	3	219	2.6	90	0.89	14	0.25	0.4
45	0.3658	0.0087	0.0498	0.0005	0.1771	317	7	313	3	157	4.2	99	2.4	15	0.39	0.6
46	0.3609	0.0072	0.0491	0.0005	0.5825	312	5	309	3	483	8.0	213	3.2	32	0.52	0.4

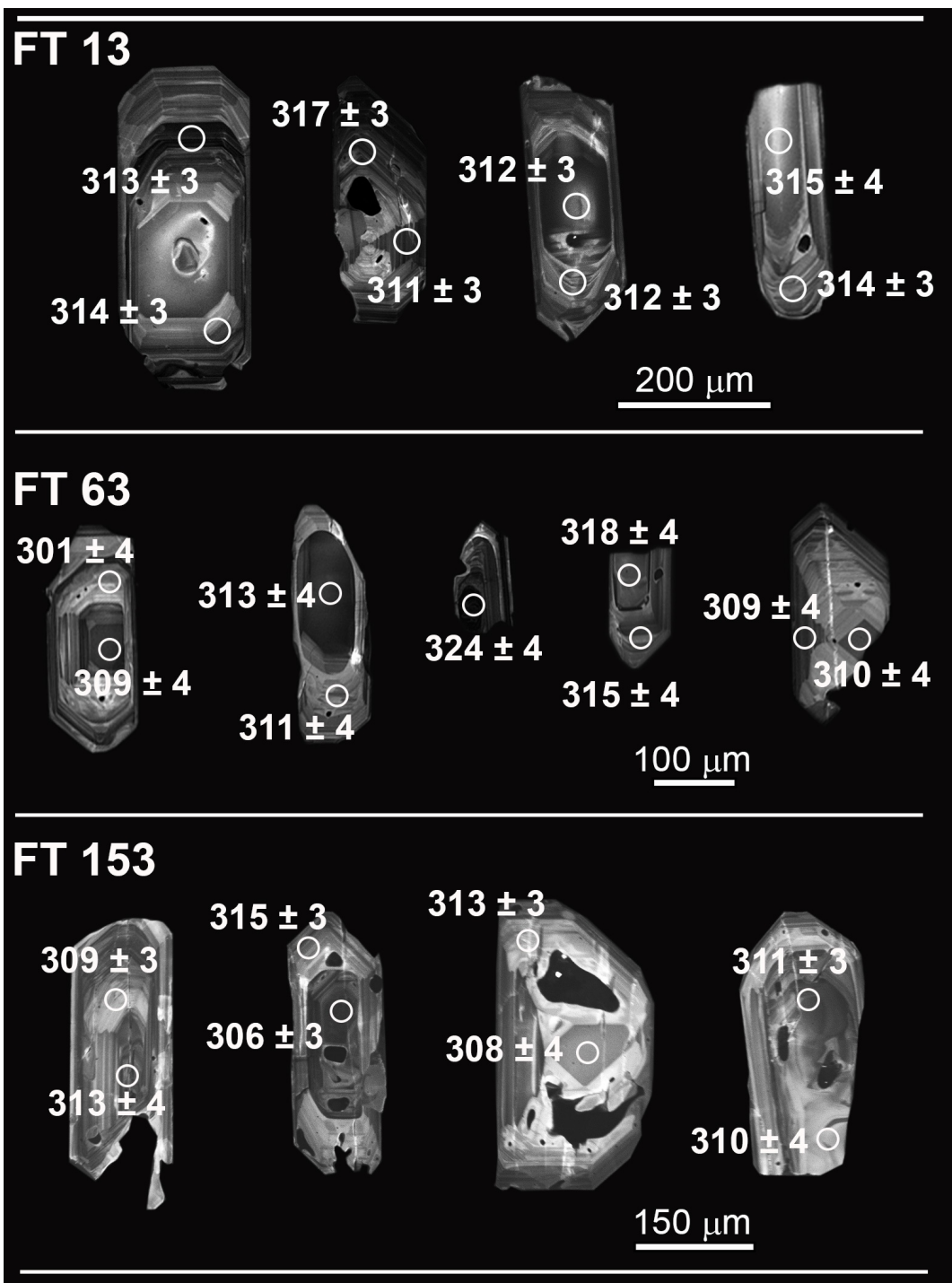
Analysis	Corrected isotope ratios					Apparent ages (Ma)					U, Th and Pb content (ppm)						
	$^{207}\text{Pb}/^{235}\text{U}$	$\pm 2\sigma$	$^{206}\text{Pb}/^{238}\text{U}$	$\pm 2\sigma$	error corr.	$^{207}\text{Pb}/^{235}\text{U}$	$\pm 2\sigma$	$^{206}\text{Pb}/^{238}\text{U}$	$\pm 2\sigma$	Approx U	$\pm 2\sigma$	Approx Th	$\pm 2\sigma$	Approx Pb	$\pm 2\sigma$	Th/U	
47	0.3736	0.0076	0.0504	0.0004	0.2894	322	6	317	3	381	14.0	203	7.5	31	1.1	0.5	
48	0.3570	0.0078	0.0495	0.0005	0.2344	311	6	311	3	192	2.6	91	1.6	14	0.35	0.5	
49	0.3623	0.0072	0.0499	0.0005	0.2146	314	5	314	3	293	2.0	127	0.7	20	0.31	0.4	
<b>Sample FT63</b>																	
1	0.3556	0.0092	0.0483	0.0007	0.2409	308	7	304	4	88	1.1	38	0.43	5.4	0.13	0.4	
2	0.3670	0.0067	0.0502	0.0006	0.2486	317	5	315	4	197	1.6	92	0.79	14.2	0.27	0.5	
3	0.3572	0.0058	0.0491	0.0006	0.3549	311	4	309	4	319	14	203	10	29	1.5	0.6	
4	0.3581	0.0062	0.0495	0.0007	0.5321	310	5	311	4	310	5.4	116	0.94	17	0.27	0.4	
5	0.3561	0.0070	0.0497	0.0007	0.5690	309	5	313	4	296	7	165	2.4	24	0.43	0.6	
6	0.3540	0.0072	0.0484	0.0008	0.5930	308	5	305	5	287	5.1	122	1.7	18	0.3	0.4	
7	0.3644	0.0067	0.0504	0.0006	0.3101	315	5	317	4	224	2.2	98	0.73	14	0.21	0.4	
8	0.3544	0.0099	0.0492	0.0007	0.1445	307	7	310	4	97	0.59	41	0.32	6.1	0.15	0.4	
9	0.3534	0.0069	0.0490	0.0006	0.2568	307	5	308	4	195	1.9	122	1	17.9	0.26	0.6	
10	0.3645	0.0058	0.0497	0.0007	0.5374	316	4	313	4	656	7.8	302	1.8	46.0	0.5	0.5	
11	0.3644	0.0056	0.0499	0.0006	0.5807	315	4	314	4	563	6.8	219	2	33.7	0.39	0.4	
12	0.3595	0.0092	0.0492	0.0007	0.1193	311	7	309	4	81	0.91	37	0.39	5.4	0.13	0.5	
13	0.3540	0.0089	0.0499	0.0007	0.2174	307	7	314	4	109	1.7	53	0.86	8.0	0.2	0.5	
14	0.3494	0.0068	0.0486	0.0006	0.2436	304	5	306	4	190	1.8	88	0.65	13	0.21	0.5	
15	0.3556	0.0085	0.0494	0.0007	0.1645	309	6	311	4	131	1.9	53	1.2	7.6	0.22	0.4	
16	0.3563	0.0056	0.0493	0.0007	0.6406	309	4	310	4	498	5.7	166	1.5	26	0.45	0.3	
17	0.3727	0.0087	0.0507	0.0007	0.2094	321	6	319	4	124	1.3	55	0.34	8.5	0.16	0.4	
18	0.3600	0.0079	0.0488	0.0006	0.2532	312	6	307	4	148	7.7	80	6.5	12	1	0.5	
19	0.3562	0.0079	0.0480	0.0006	0.2687	310	6	302	4	116	1.5	54	0.57	8.1	0.16	0.5	
20	0.3709	0.0064	0.0500	0.0007	0.6079	321	5	315	4	536	32	352	29	55	4.1	0.7	
21	0.3611	0.0075	0.0492	0.0008	0.5536	312	6	309	5	266	13	132	7.5	20	1	0.5	
22	0.3643	0.0064	0.0501	0.0006	0.1454	315	5	315	4	226	3.1	110	1.4	17	0.28	0.5	
23	0.3732	0.0083	0.0506	0.0007	0.3398	322	6	318	4	140	5.1	81	3.3	13	0.5	0.6	
24	0.3713	0.0068	0.0500	0.0006	0.3588	321	5	315	4	233	2.4	110	1.2	16	0.33	0.5	
25	0.3587	0.0093	0.0492	0.0006	0.2232	311	7	310	4	96	1.3	44	0.53	6.7	0.17	0.5	
26	0.3633	0.0075	0.0490	0.0006	0.1746	315	6	309	4	176	2	95	0.91	14	0.22	0.5	
27	0.3571	0.0068	0.0490	0.0007	0.4754	310	5	309	4	322	7.3	168	4.4	25	0.72	0.5	
28	0.3560	0.0064	0.0479	0.0007	0.5673	309	5	301	4	429	6.9	172	1.8	26	0.35	0.4	
29	0.3648	0.0071	0.0504	0.0006	0.2223	315	5	317	4	177	2.1	84	0.81	13	0.23	0.5	
30	0.3482	0.0078	0.0484	0.0006	0.2183	303	6	305	4	126	1.8	70	0.89	10	0.19	0.6	
31	0.3574	0.0099	0.0490	0.0007	0.2362	310	7	308	4	110	2.5	56	1.6	8.1	0.28	0.5	
32	0.3636	0.0084	0.0487	0.0007	0.1358	316	6	307	4	104	0.94	42	0.31	6.0	0.15	0.4	
33	0.3590	0.0070	0.0484	0.0006	0.3192	311	5	305	4	243	2.2	100	0.77	16	0.25	0.4	
34	0.3652	0.0080	0.0498	0.0007	0.4030	316	6	314	4	191	3.6	91	1.1	14	0.26	0.5	
35	0.3593	0.0057	0.0494	0.0007	0.5145	311	4	311	4	618	8.2	211	2.3	34	0.48	0.3	
36	0.3763	0.0073	0.0509	0.0007	0.2244	324	5	320	4	191	2.5	80	1	13	0.25	0.4	
37	0.3637	0.0071	0.0496	0.0006	0.1349	316	5	312	4	170	2	75	0.7	12	0.21	0.4	
38	0.3507	0.0065	0.0480	0.0007	0.3379	305	5	302	4	196	4.4	103	3.4	16	0.55	0.5	
39	0.3601	0.0066	0.0503	0.0007	0.3578	314	5	317	4	200	2	78	0.75	12	0.28	0.4	
40	0.3706	0.0079	0.0504	0.0006	0.2422	320	6	317	4	171	1.6	90	0.61	14	0.23	0.5	
41	0.3667	0.0065	0.0498	0.0006	0.2774	317	5	313	4	243	1.9	137	1.7	21	0.43	0.6	
42	0.3635	0.0070	0.0493	0.0006	0.3216	314	5	310	4	239	2.1	132	0.95	20	0.34	0.6	
43	0.3753	0.0061	0.0515	0.0007	0.6098	323	5	324	4	562	9.2	277	3	44	0.54	0.5	
44	0.3649	0.0070	0.0493	0.0006	0.2936	316	5	310	4	213	2	126	1.3	19	0.32	0.6	

Analysis	Corrected isotope ratios						Apparent ages (Ma)				U, Th and Pb content (ppm)					
	$^{207}\text{Pb}/^{235}\text{U}$	$\pm 2\sigma$	$^{206}\text{Pb}/^{238}\text{U}$	$\pm 2\sigma$	error corr.	$^{207}\text{Pb}/^{235}\text{U}$	$\pm 2\sigma$	$^{206}\text{Pb}/^{238}\text{U}$	$\pm 2\sigma$	Approx U	$\pm 2\sigma$	Approx Th	$\pm 2\sigma$	Approx Pb	$\pm 2\sigma$	Th/U
45	0.3641	0.0074	0.0498	0.0007	0.4997	316	6	313	4	358	6.6	119	1.3	18	0.37	0.3
46	0.3682	0.0070	0.0498	0.0006	0.2235	318	5	313	4	224	4.3	144	2.3	22	0.39	0.6
47	0.3576	0.0086	0.0494	0.0006	0.1885	310	7	311	4	126	1.5	59	0.61	8.8	0.19	0.5
48	0.3660	0.0130	0.0499	0.0008	0.1315	317	10	314	5	56	1.5	23	0.8	3.5	0.15	0.4
49	0.3574	0.0100	0.0496	0.0007	0.1897	310	8	312	4	87	1.5	39	0.41	6.1	0.18	0.5
50	0.3560	0.0120	0.0488	0.0008	0.0497	309	9	307	5	62	1.3	27	0.73	4.2	0.16	0.4
51	0.3630	0.0062	0.0503	0.0007	0.6300	314	5	316	4	642	13	229	3.6	36	0.57	0.4
52	0.3619	0.0073	0.0494	0.0006	0.2395	313	5	311	4	191	2.3	89	0.78	14	0.27	0.5
53	0.3553	0.0100	0.0490	0.0007	0.1803	309	8	308	4	86	1.2	45	0.48	6.7	0.16	0.5
54	0.3668	0.0065	0.0501	0.0006	0.2709	317	5	315	4	268	3.1	124	1.2	19	0.33	0.5
55	0.3502	0.0073	0.0496	0.0006	0.2128	305	5	312	4	190	3	109	3	17	0.56	0.6
56	0.3583	0.0094	0.0496	0.0006	0.0850	311	7	312	4	94	1.5	45	0.68	6.9	0.18	0.5
57	0.3607	0.0063	0.0490	0.0006	0.3257	314	5	308	4	240	5.8	129	3.2	20	0.51	0.5
<b>Sample FT153</b>																
1	0.3519	0.0087	0.0483	0.0006	0.3909	306	7	304	4	139	1.1	82	1.1	12	0.3	0.6
2	0.3570	0.0088	0.0492	0.0006	0.2163	310	7	310	4	97	1.1	40	0.39	6.0	0.2	0.4
3	0.3598	0.0076	0.0500	0.0005	0.1115	312	6	315	3	149	5.3	87	2.7	13	0.4	0.6
4	0.3630	0.0065	0.0503	0.0005	0.2937	314	5	316	3	194	1.4	68	0.4	10	0.2	0.3
5	0.3682	0.0065	0.0505	0.0006	0.6099	318	5	317	4	532	7.1	174	1.6	28	0.4	0.3
6	0.3683	0.0068	0.0509	0.0005	0.3373	318	5	320	3	223	3.9	80	1.2	12	0.3	0.4
7	0.3736	0.0080	0.0505	0.0005	0.3383	322	6	317	3	150	2.4	77	1.2	12	0.3	0.5
8	0.3626	0.0068	0.0493	0.0007	0.5102	314	5	310	4	307	5.5	133	1.7	20	0.3	0.4
9	0.3672	0.0089	0.0499	0.0005	0.1776	316	7	314	3	102	2.1	57	1.3	8.4	0.2	0.6
10	0.3541	0.0096	0.0493	0.0006	0.2095	307	7	310	4	98	1.3	52	1.4	7.4	0.3	0.5
11	0.3650	0.0120	0.0497	0.0006	0.0432	315	9	312	4	61	1.3	26	0.66	4.0	0.1	0.4
12	0.3661	0.0063	0.0498	0.0006	0.5100	317	5	313	4	436	5.6	184	1.6	27	0.3	0.4
13	0.3691	0.0085	0.0506	0.0006	0.2843	319	6	318	4	134	1.2	64	0.72	9.6	0.2	0.5
14	0.3661	0.0091	0.0499	0.0005	0.1086	316	7	314	3	85	0.9	47	0.35	7.2	0.1	0.6
15	0.3652	0.0064	0.0499	0.0004	0.3671	316	5	314	3	240	4.3	83	1.2	12	0.2	0.3
16	0.3564	0.0059	0.0488	0.0005	0.5983	310	5	307	3	402	5.3	168	1.3	25	0.3	0.4
17	0.3634	0.0063	0.0493	0.0006	0.5385	314	5	310	4	393	6	147	2.9	22	0.5	0.4
18	0.3593	0.0072	0.0491	0.0006	0.5847	311	5	309	4	339	4.8	210	2.3	33	0.4	0.6
19	0.3672	0.0083	0.0495	0.0006	0.2518	318	6	312	4	168	1.3	77	0.54	11	0.2	0.5
20	0.3635	0.0075	0.0493	0.0006	0.3249	316	6	310	4	190	2.2	88	0.87	13	0.2	0.5
21	0.3635	0.0062	0.0500	0.0005	0.2800	315	5	314	3	236	2.8	97	0.78	14	0.2	0.4
22	0.3602	0.0071	0.0488	0.0006	0.5660	312	5	307	4	256	6.3	79	1.5	12	0.3	0.3
23	0.3619	0.0071	0.0499	0.0005	0.3379	314	5	314	3	203	2.3	78	0.74	12	0.2	0.4
24	0.3519	0.0074	0.0482	0.0005	0.2615	306	6	303	3	148	2.2	58	1.5	8.2	0.3	0.4
25	0.3681	0.0058	0.0504	0.0005	0.6445	319	4	317	3	573	9	221	2.2	34	0.4	0.4
26	0.3496	0.0087	0.0486	0.0005	0.1698	304	7	306	3	90	1.1	38	0.37	5.5	0.1	0.4
27	0.3607	0.0070	0.0497	0.0005	0.2853	313	5	312	3	158	1.5	95	0.68	14	0.2	0.6
28	0.3660	0.0060	0.0501	0.0005	0.5732	317	5	315	3	397	8.8	165	3.4	25	0.5	0.4
29	0.3738	0.0070	0.0506	0.0005	0.2777	322	5	318	3	182	2.4	77	0.78	11	0.2	0.4
30	0.3605	0.0064	0.0500	0.0006	0.5463	313	5	315	4	323	6.6	126	1.6	19	0.3	0.4
31	0.3637	0.0067	0.0499	0.0005	0.2722	314	5	314	3	207	2.9	73	0.93	11	0.2	0.4
32	0.3607	0.0062	0.0497	0.0006	0.5652	312	5	313	3	357	4.3	160	1.1	24	0.3	0.4
33	0.3610	0.0060	0.0492	0.0005	0.5441	313	5	310	3	536	9.3	224	2.7	34	0.5	0.4
34	0.3624	0.0064	0.0494	0.0005	0.3932	314	5	311	3	286	2.1	115	0.72	18	0.3	0.4

Analysis	Corrected isotope ratios						Apparent ages (Ma)				U, Th and Pb content (ppm)					
	$^{207}\text{Pb}/^{235}\text{U}$	$\pm 2\sigma$	$^{206}\text{Pb}/^{238}\text{U}$	$\pm 2\sigma$	error corr.	$^{207}\text{Pb}/^{235}\text{U}$	$\pm 2\sigma$	$^{206}\text{Pb}/^{238}\text{U}$	$\pm 2\sigma$	Approx U	$\pm 2\sigma$	Approx Th	$\pm 2\sigma$	Approx Pb	$\pm 2\sigma$	Th/U
35	0.3553	0.0084	0.0493	0.0006	0.2080	308	6	310	4	102	1.6	48	0.95	7.4	0.2	0.5
36	0.3677	0.0079	0.0502	0.0005	0.1629	318	6	316	3	140	1.8	61	0.69	9.4	0.2	0.4
37	0.3659	0.0067	0.0501	0.0004	0.2600	318	5	316	3	184	5.7	73	2.7	12	0.4	0.4
38	0.3633	0.0063	0.0502	0.0005	0.3690	314	5	316	3	240	2.3	101	0.83	16	0.2	0.4
39	0.3537	0.0063	0.0482	0.0005	0.2228	307	5	304	3	186	1.5	81	0.93	12	0.2	0.4
40	0.3568	0.0076	0.0490	0.0005	0.1728	310	6	308	3	128	2.1	84	1.8	12	0.3	0.7
41	0.3553	0.0086	0.0496	0.0006	0.2048	308	6	312	3	125	1.4	64	0.72	9.7	0.2	0.5
42	0.3583	0.0092	0.0496	0.0006	0.3345	311	7	312	3	118	1	73	0.8	11	0.3	0.6
43	0.3473	0.0080	0.0486	0.0005	0.3254	303	6	306	3	122	1.4	81	0.75	11	0.2	0.7
44	0.3519	0.0061	0.0490	0.0006	0.5591	307	5	309	3	459	12	127	2.6	18	0.5	0.3
45	0.3510	0.0057	0.0482	0.0005	0.4878	305	4	303	3	511	8.2	181	3	27	0.4	0.4
46	0.3641	0.0076	0.0501	0.0007	0.5464	316	6	315	4	275	17	159	9.3	24	1.2	0.6
47	0.3577	0.0074	0.0488	0.0005	0.3002	310	6	307	3	182	1.5	97	0.99	14	0.3	0.5
48	0.3596	0.0100	0.0497	0.0007	0.2772	311	7	313	4	88	1	48	0.48	7.1	0.2	0.5
49	0.3595	0.0082	0.0491	0.0005	0.3158	311	6	309	3	123	1.3	74	0.52	11	0.2	0.6
50	0.3509	0.0085	0.0484	0.0005	0.3031	305	6	305	3	109	1.6	67	0.77	9.7	0.2	0.6
51	0.3750	0.0077	0.0511	0.0005	0.3163	323	6	321	3	173	2.4	113	1	17	0.3	0.7
52	0.3557	0.0063	0.0487	0.0005	0.5088	309	5	306	3	344	8.7	208	4.2	32	0.7	0.6
53	0.3657	0.0073	0.0501	0.0005	0.2821	316	5	315	3	133	1.9	62	0.68	9.5	0.2	0.5
54	0.3569	0.0100	0.0490	0.0006	0.3371	309	8	308	4	90	2.6	56	1.9	8.4	0.3	0.6
55	0.3616	0.0076	0.0498	0.0005	0.3562	313	6	313	3	135	2.2	62	0.86	9.7	0.2	0.5
56	0.3661	0.0068	0.0499	0.0005	0.4413	316	5	314	3	227	2.6	102	1.4	16	0.3	0.4
57	0.3691	0.0088	0.0504	0.0006	0.3185	319	7	317	3	134	1.2	64	0.47	9.8	0.2	0.5
58	0.3521	0.0076	0.0486	0.0005	0.3491	306	6	306	3	141	0.97	61	0.49	9.4	0.2	0.4
59	0.3628	0.0071	0.0493	0.0005	0.3754	314	5	310	3	215	4.4	151	3.3	23	0.6	0.7
60	0.3540	0.0074	0.0487	0.0005	0.2421	307	6	307	3	134	1.2	68	0.5	10	0.2	0.5
61	0.3504	0.0087	0.0485	0.0006	0.0874	304	7	305	4	85	1.3	49	1.4	7.5	0.3	0.6

## DATA REPOSITORY ITEM 4

Cathodoluminescence images of representative zircon grains



## Data Repository Item 5

### ANISOTROPY OF MAGNETIC SUSCEPTIBILITY

#### Detailed methodology

The sampling involved both the in-situ drilling of rock cores using a hand-held gasoline drill and collecting oriented block samples. The latter were then drilled perpendicularly to the orientation plane at a laboratory table drill, and the core orientations were recalculated accordingly.

In order to precisely determine the source of AMS signal, variations of bulk susceptibility with temperature ( $k_b-T$ ) were obtained using a CS-L Cryostat and a CS4 non-magnetic Furnace units connected to an Agico MFK1-A Kappabridge in the Laboratory of Rock Magnetism, Institute of Geology and Paleontology, Charles University in Prague (Hrouda, 1994; Hrouda et al., 1997; Jelínek and Pokorný, 1997). Thermomagnetic curves in the range of  $-196$  °C to  $700$  °C were acquired in two steps. First, the specimens were cooled down to the temperature of liquid nitrogen (ca.  $-196$  °C) and heated up to room temperature ( $\sim 20$  °C; LT heating curve). Second, all specimens were heated up from the room temperature to  $700$  °C (HT heating curve) and spontaneously cooled down to room temperature (HT cooling curve) at a rate of  $\sim 14$  °C/min. The resulting thermomagnetic curves were analyzed in the Cureval 8 program ([www.agico.com](http://www.agico.com); Hrouda et al., 1997) using the following procedures: (1) the Curie temperatures ( $T_c$ ) were determined by a method of Petrovský and Kapička (2006), and (2) the relative fraction of ferromagnetic s.l. and paramagnetic components (ferro/para resolution) was estimated using the method of Hrouda (1994).

In addition, we determine the size of magnetic grains using the frequency-dependent bulk susceptibility method (e.g., Le Borgne, 1955; Dearing et al., 1996; Maher and Thompson, 1999; Hrouda, 2011; Chlupáčová et al., 2012; Hrouda and Ježek, 2014; Hrouda et al., 2018). The representative specimens were measured on a multi-frequency MFK1-FA

Kappabridge (Institute of Geophysics, Czech Academy of Sciences) in the field 200 A/m at three operating frequencies at room temperature. Provided that the frequency-dependent susceptibility was obtained at three different frequencies, here we use three  $X_{FD}$  parameters defined as  $X_{1,4}$ ,  $X_{4,16}$ , and  $X_{1,16}$  for low to high frequency ratios of 976/3904 Hz, 3904/15616 Hz, and 976/15616 Hz, respectively (see details in Chlupáčová et al., 2012).

The magnetic fabrics and parameters were measured using a MFK1-A Kappabridge apparatus (Jelínek and Pokorný, 1997) equipped with a 3D rotator (Studýnka et al., 2014) in the field of 200 A/m for a frequency of 976 Hz (Laboratory of Rock Magnetism, Institute of Geology and Paleontology, Charles University in Prague). A statistical analysis of the data was treated using the ANISOFT 4.2 software (Jelínek, 1978; Hrouda et al., 1990; Chadima and Jelínek, 2008;).

The AMS tensor is represented by an ellipsoid with the principal susceptibility axes  $k_1 \geq k_2 \geq k_3$  where the maximum susceptibility ( $k_1$ ) represents magnetic lineation and the minimum susceptibility ( $k_3$ ) characterize the pole to magnetic foliation. The AMS can be further described by several parameters (Tarling and Hrouda, 1993) from which we use (1) the bulk or mean susceptibility ( $k_b = (k_1 + k_2 + k_3)/3$ ) reflecting the type and volume fraction of magnetic minerals, (2) the degree of anisotropy ( $P = k_1/k_3$ ) which indicates the eccentricity of the AMS ellipsoid and may be thus related to the intensity of the shape-preferred orientation of magnetic minerals (Nagata, 1962), and (3) the shape parameter ( $T = 2\ln(k_2/k_3)/\ln(k_1/k_3) - 1$ ) which describes symmetry of the AMS ellipsoid. For  $-1 \leq T < -0.050$  the ellipsoid is prolate, for  $T \approx 0$  neutral, and for  $1 \geq T > 0.050$  oblate (Jelínek, 1981; for the purpose of this paper, we consider cut-off the neutral ellipsoids as those ranging from  $-0.050$  to  $0.050$ ).

## REFERENCES

- Dearing, J.A., Dann, R.J.L., Hay, K., Lees, J.A., Loveland, P.J., Maher, B.A., O'Grady, K., 1996. Frequency-dependent susceptibility measurements of environmental materials. *Geophysical Journal International* 124, 228–240.

- Hrouda, F., 2011. Models of frequency-dependent susceptibility of rocks and soils revisited and broadened. *Geophysical Journal International* 187, 1259–1269.
- Hrouda, F., 1994. A technique for the measurement of thermal changes of magnetic susceptibility of weakly magnetic rocks by the CS-2 apparatus and KLY-2 Kappabridge. *Geophysical Journal International* 118, 604–612
- Hrouda, F., Chadima, M., Ježek, J., Kadlec, J., 2018. Anisotropies of in-phase, out-of-phase, and frequency-dependent susceptibilities in three loess/palaeosol profiles in the Czech Republic; methodological implications. *Studia Geophysica et Geodaetica* 62, 1–19.
- Hrouda, F., Jelínek, V., Hrušková, L., 1990. A package of programs for statistical evaluation of magnetic data using IBM-PC computers. *Eos Transactions American Geophysical Union* 71, 1289.
- Hrouda, F., Jelínek, V., Zapletal, K., 1997. Refined technique for susceptibility resolution into ferromagnetic and paramagnetic components based on susceptibility temperature-variation measurement. *Geophysical Journal International* 129, 715–719.
- Hrouda, F., Ježek, J., 2014. Frequency-dependent AMS of rocks: A tool for the investigation of the fabric of ultrafine magnetic particles. *Tectonophysics* 629, 27–38.
- Chadima, M., Jelínek, V., 2008. Anisoft 4.2. – anisotropy data browser, in: Paleo, Rock and Environmental Magnetism 11th Castle Meeting, Contributions to Geophysics and Geodesy 38. p. 41.
- Chlupáčová, M., Hrouda, F., Nižnanský, D., Procházka, V., Petáková, Z., Laufek, F., 2012. Frequency-dependent susceptibility and other magnetic properties of Celtic and Mediaeval graphitic pottery from Bohemia: An introductory study. *Studia Geophysica et Geodaetica* 56, 803–825.
- Jelínek, V., 1981. Characterization of the magnetic fabric of rocks. *Tectonophysics* 79, T63–T67.

- Jelínek, V., 1978. Statistical processing of anisotropy of magnetic susceptibility measured on groups of specimens. *Studia Geophysica et Geodaetica* 22, 50–62.
- Jelínek, V., Pokorný, J., 1997. Some new concepts in technology of transformer bridges for measuring susceptibility anisotropy of rocks. *Physics and Chemistry of the Earth* 22, 179–181.
- Jelínek, V., Pokorný, J., 1997. Some new concepts in technology of transformer bridges for measuring susceptibility anisotropy of rocks. *Physics and Chemistry of the Earth* 22, 179–181.
- Le Borgne, E., 1955. Susceptibilité magnétique anormale du sol superficiel. *Annales de géophysique* 11, 399–419.
- Maher, B.A., Thompson, R., 1999. Quaternary climates, environments and magnetism. Cambridge University Press, New York, 412 pp.
- Nagata, T., 1962. Rock Magnetism. Maruzen, Tokyo.
- Petrovský, E.D., Kapička, A., 2006. On determination of the Curie point from thermomagnetic curves. *Journal of Geophysical Research: Solid Earth* 111, B12S27.  
<http://dx.doi.org/doi:10.1029/2006JB004507>
- Studýnka, J., Chadima, M., Suza, P., 2014. Fully automated measurement of anisotropy of magnetic susceptibility using 3D rotator. *Tectonophysics* 629, 6–13.
- Tarling, D., Hrouda, F., 1993. Magnetic Anisotropy of Rocks. Chapman & Hall, London.

## Data Repository Item 6

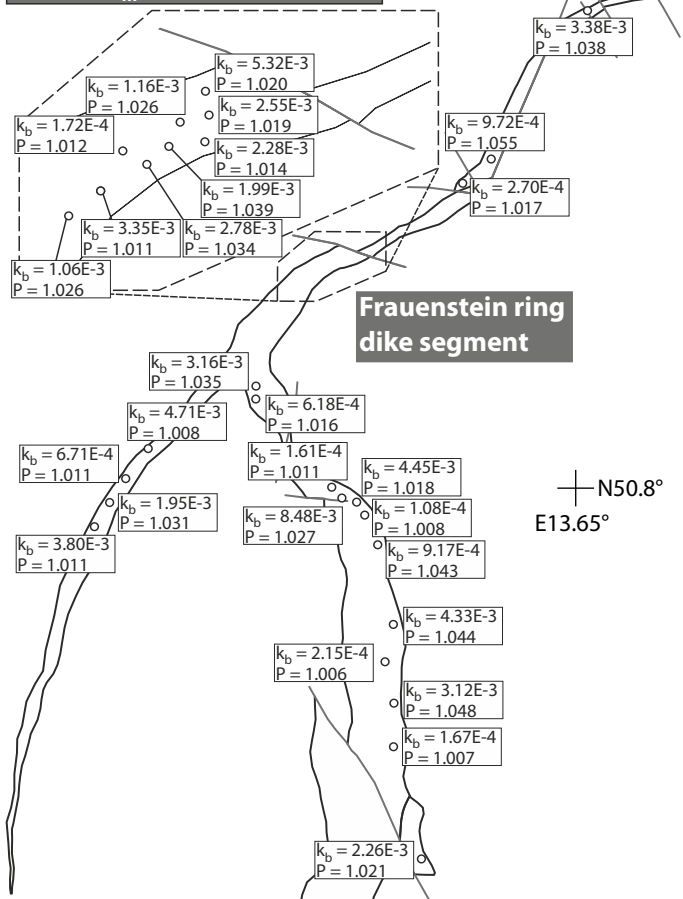
AMS station mean data (Loučná-Fláje segment)																		
Station	Granite facies	Latitude (N)	Longitude (E)	N <sub>t</sub>	N <sub>a</sub>	N <sub>c</sub>	K <sub>b</sub>	P	P <sub>j</sub>	T	K <sub>1d</sub>	K <sub>1i</sub>	C <sub>1a</sub>	C <sub>1b</sub>	K <sub>3d</sub>	K <sub>3i</sub>	C <sub>3a</sub>	C <sub>3b</sub>
<b>FT013</b>	2	50.695550	13.586360	13	13	5	3.95E-03	1.043	1.045	0.433	231	70	11	5	111	11	11	4
<b>FT014</b>	2	50.691710	13.584780	10	10	4	2.75E-04	1.018	1.019	0.158	133	55	46	6	228	4	19	13
<b>FT066</b>	1	50.685920	13.589150	10	10	5	1.06E-02	1.027	1.027	0.048	322	66	11	4	195	15	9	5
<b>FT068</b>	1	50.683700	13.591700	13	11	6	5.56E-04	1.009	1.010	0.230	288	66	31	16	47	12	41	15
<b>FT098</b>	2	50.635740	13.611197	12	12	4	4.61E-03	1.028	1.028	-0.153	56	18	5	5	320	18	11	3
<b>FT099</b>	2	50.647167	13.610880	9	9	4	4.20E-03	1.038	1.038	0.001	34	43	10	4	129	5	8	5
<b>FT100</b>	1	50.707251	13.585867	12	11	5	2.05E-03	1.021	1.021	-0.131	30	76	12	5	279	5	24	6
<b>FT159</b>	1	50.607567	13.623199	16	16	6	1.60E-04	1.007	1.007	0.239	149	8	17	9	242	25	12	5
<b>FT160</b>	1	50.663343	13.600603	9	9	3	5.69E-03	1.032	1.032	-0.031	62	7	9	6	329	28	8	6
<b>FT161</b>	1	50.663590	13.601902	13	13	4	4.88E-03	1.016	1.017	0.218	13	63	23	6	110	4	12	6
<b>Hermsdorf segment</b>																		
<b>FT102</b>	1	50.725577	13.602925	14	13	5	2.37E-04	1.023	1.023	0.176	23	67	33	4	247	17	34	11
<b>FT103</b>	1	50.731142	13.596890	8	7	3	1.85E-04	1.010	1.011	0.104	308	59	35	21	60	13	37	8
<b>FT104</b>	1	50.730801	13.600779	14	12	5	2.44E-04	1.007	1.007	0.121	317	28	23	9	74	40	26	8
<b>FT118</b>	1	50.803270	13.603875	8	8	4	9.17E-04	1.043	1.047	0.785	238	26	35	4	330	5	6	3
<b>FT119</b>	1	50.807917	13.600650	10	9	4	1.80E-04	1.008	1.008	0.083	269	54	26	13	26	18	23	11
<b>FT120</b>	2	50.809994	13.597870	13	13	5	4.45E-03	1.018	1.018	0.086	184	70	8	4	37	17	16	4
<b>FT121</b>	2	50.810297	13.595738	10	10	5	1.61E-04	1.011	1.012	-0.169	129	64	41	5	36	2	10	5
<b>FT122</b>	2	50.811326	13.594937	12	10	5	8.48E-03	1.027	1.028	-0.242	111	69	12	4	294	21	12	4
<b>FT123</b>	2	50.792081	13.607638	9	8	5	4.33E-03	1.044	1.046	0.466	36	25	30	7	301	11	11	1
<b>FT124</b>	1	50.786553	13.605565	11	10	6	2.15E-04	1.006	1.006	0.018	56	17	16	8	148	7	24	8
<b>FT125</b>	2	50.780879	13.607734	11	11	5	3.12E-03	1.048	1.049	0.266	225	33	10	5	128	11	5	3
<b>FT126</b>	1	50.759371	13.614515	14	14	5	1.67E-04	1.007	1.007	0.016	136	13	58	30	45	2	33	25
<b>FT127</b>	2	50.842493	13.711469	14	14	6	2.26E-03	1.021	1.022	-0.394	227	9	16	4	318	3	11	5
<b>FT158</b>	1	50.730244	13.604645	19	19	8	4.06E-03	1.010	1.010	0.001	236	11	42	35	140	28	81	36
<b>Frauenstein segment</b>																		
<b>FT107</b>	1	50.857480	13.627527	14	12	6	2.70E-04	1.017	1.017	-0.434	108	40	16	11	8	12	31	12
<b>FT108</b>	2	50.854187	13.620235	13	13	5	9.72E-04	1.055	1.058	-0.576	67	48	21	2	325	11	33	18
<b>FT109A</b>	1	50.843117	13.593488	8	8	4	2.28E-03	1.014	1.015	0.338	307	49	36	5	173	31	7	3
<b>FT109B</b>	1	50.844122	13.593441	9	9	4	2.55E-03	1.019	1.020	-0.321	274	22	13	5	12	19	22	5
<b>FT109C</b>	1	50.8444854	13.592968	10	10	4	5.32E-03	1.020	1.020	0.020	337	31	9	4	188	55	11	6
<b>FT110</b>	1	50.839778	13.586400	10	10	5	1.06E-03	1.026	1.027	-0.528	136	42	12	6	7	35	19	8
<b>FT111</b>	1	50.840785	13.588225	10	10	4	3.35E-03	1.011	1.011	0.111	348	26	21	6	184	63	24	9
<b>FT112</b>	1	50.842038	13.590440	11	11	6	2.78E-03	1.034	1.036	0.523	101	31	30	3	3	14	5	4
<b>FT113</b>	1	50.843663	13.591889	13	11	7	1.16E-03	1.026	1.027	0.507	238	22	27	4	340	28	14	3
<b>FT114</b>	2	50.842800	13.591527	9	9	4	1.99E-03	1.039	1.040	0.118	111	48	8	5	317	39	7	3

Station	Granite facies	Latitude (N)	Longitude (E)	N <sub>t</sub>	N <sub>a</sub>	N <sub>c</sub>	K <sub>b</sub>	P	P <sub>j</sub>	T	K <sub>1d</sub>	K <sub>1i</sub>	C <sub>1a</sub>	C <sub>1b</sub>	K <sub>3d</sub>	K <sub>3i</sub>	C <sub>3a</sub>	C <sub>3b</sub>
<b>FT115</b>	1	50.842161	13.589153	9	9	4	1.72E-04	1.012	1.012	0.288	92	36	82	10	188	9	17	6
<b>FT116</b>	2	50.824878	13.575356	8	8	4	3.16E-03	1.035	1.035	-0.260	31	17	5	3	296	16	5	4
<b>FT117</b>	2	50.823298	13.575391	9	8	4	6.18E-04	1.016	1.017	0.613	42	46	35	5	272	32	7	5
<b>FT150</b>	2	50.805150	13.540230	13	13	5	6.71E-04	1.011	1.011	0.353	60	7	14	3	313	65	8	3
<b>FT151</b>	1	50.808500	13.543550	14	12	6	3.80E-03	1.011	1.012	0.377	209	45	30	4	309	10	6	4
<b>FT152</b>	2	50.816360	13.551810	11	11	4	1.95E-03	1.031	1.031	-0.051	244	47	6	5	115	30	11	5
<b>FT153</b>	2	50.873834	13.656114	13	12	5	4.71E-03	1.008	1.008	-0.341	115	45	6	4	15	10	34	5
<b>FT154</b>	1	50.807028	13.759528	9	9	4	3.83E-03	1.038	1.040	0.486	131	29	9	3	229	14	5	3
<b>Altenberg segment</b>																		
<b>FT063</b>	1	50.869000	13.688090	19	17	6	4.08E-05	1.018	1.018	0.145	346	11	27	12	253	17	14	7
<b>FT128</b>	3	50.842408	13.713382	19	19	7	1.23E-04	1.009	1.009	0.337	273	14	22	5	4	4	11	5
<b>FT129</b>	1	50.842360	13.729670	10	8	5	1.80E-04	1.014	1.014	0.290	101	6	27	10	211	74	12	4
<b>FT130</b>	1	50.837115	13.737491	10	9	5	1.18E-04	1.008	1.008	-0.405	147	36	20	19	271	37	39	10
<b>FT131</b>	2	50.816620	13.723760	9	9	5	2.11E-04	1.016	1.017	0.339	23	32	27	5	224	56	10	3
<b>FT132</b>	3	50.812384	13.729383	10	10	4	1.10E-04	1.007	1.008	-0.229	142	11	13	4	233	10	16	4
<b>FT133</b>	3	50.801127	13.739788	12	12	5	1.96E-04	1.009	1.010	-0.004	324	6	9	7	224	60	12	6
<b>FT134</b>	1	50.792551	13.770820	11	11	5	2.22E-03	1.021	1.021	0.232	237	71	16	6	343	5	14	5
<b>FT135</b>	1	50.796502	13.769983	11	10	5	1.56E-04	1.011	1.011	-0.051	62	14	21	13	194	70	23	11
<b>FT136</b>	1	50.792413	13.750155	11	8	5	2.32E-04	1.019	1.019	-0.211	302.	28	39	9	207	9	26	12
<b>FT137</b>	1	50.784971	13.775035	13	13	5	4.41E-03	1.031	1.033	-0.572	73	41	8	5	189	27	16	5
<b>FT138</b>	1	50.779642	13.773657	8	8	4	2.52E-03	1.033	1.033	-0.122	248	68	11	3	69	22	14	5
<b>FT139</b>	1	50.781410	13.772946	11	11	5	1.26E-02	1.019	1.020	0.472	40	75	18	8	292	5	8	5
<b>FT140</b>	1	50.787836	13.781936	12	11	6	1.61E-04	1.005	1.005	0.154	235	7	22	11	328	21	55	12
<b>FT141</b>	1	50.750117	13.798549	12	12	4	3.13E-03	1.024	1.024	-0.022	1	88	17	5	252	1	8	6
<b>FT142</b>	1	50.771345	13.791653	9	9	4	2.03E-04	1.007	1.007	-0.003	15	67	35	19	230	19	25	20
<b>FT143</b>	1	50.762780	13.789799	17	17	7	2.36E-04	1.012	1.012	0.105	327	12	16	9	60	13	11	7
<b>FT144</b>	1	50.765736	13.797237	12	11	6	2.59E-04	1.009	1.010	-0.022	130	8	21	9	221	11	33	16
<b>FT146</b>	2	50.749445	13.782116	13	13	5	4.81E-03	1.031	1.033	-0.567	34	39	7	3	263	40	18	4
<b>FT147</b>	1	50.760156	13.776677	14	14	6	4.92E-03	1.031	1.032	0.345	52	82	19	6	295	4	13	6
<b>FT148</b>	1	50.764883	13.777747	10	8	4	2.06E-03	1.008	1.008	0.050	32	73	30	23	196	17	39	19
<b>FT149</b>	1	50.811940	13.547060	15	13	6	1.60E-04	1.014	1.014	0.239	251	40	29	10	10	30	24	8
<b>FT155</b>	1	50.801450	13.762480	14	13	6	2.00E-04	1.009	1.009	-0.081	259	21	32	13	6	37	26	13

Note: N<sub>t</sub> - total number of specimens (N = 759); N<sub>a</sub> - number of accepted specimens for AMS analyses (N = 731); N<sub>c</sub> - number of cores drilled per station (N = 322); 1 - Kfs porphyritic coarse-grained microgranite; 2 - Qz and Kfs porphyritic fine-grained microgranite; 3 - Qz porphyritic fine- to medium-grained microgranite

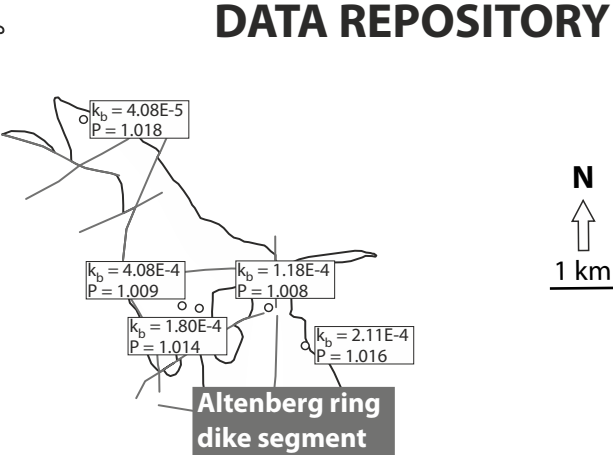
# DATA REPOSITORY ITEM 7

**Map of  $k_m$  and P parameters**



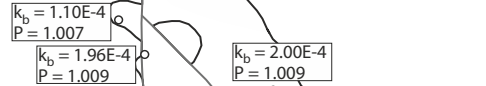
**Frauenstein ring  
dike segment**

N50.8°  
E13.65°



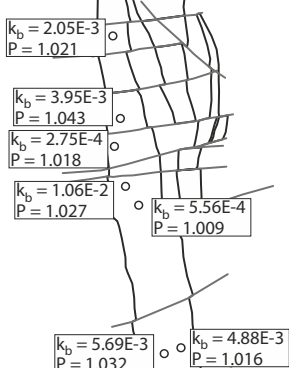
**Altenberg ring  
dike segment**

N  
1 km



**Hermsdorf ring  
dike segment**

N50.7°  
E13.65°



**Loučná-Fláje  
ring dike segment**

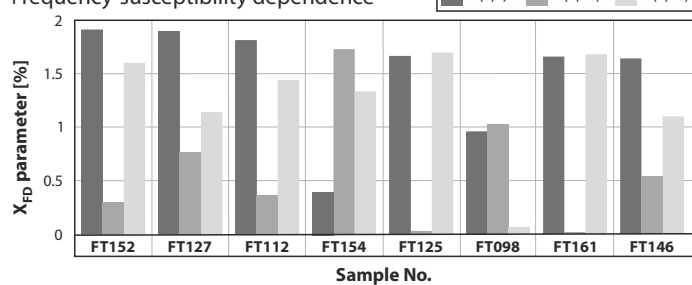
N50.6°  
E13.65°



## DATA REPOSITORY ITEM 8

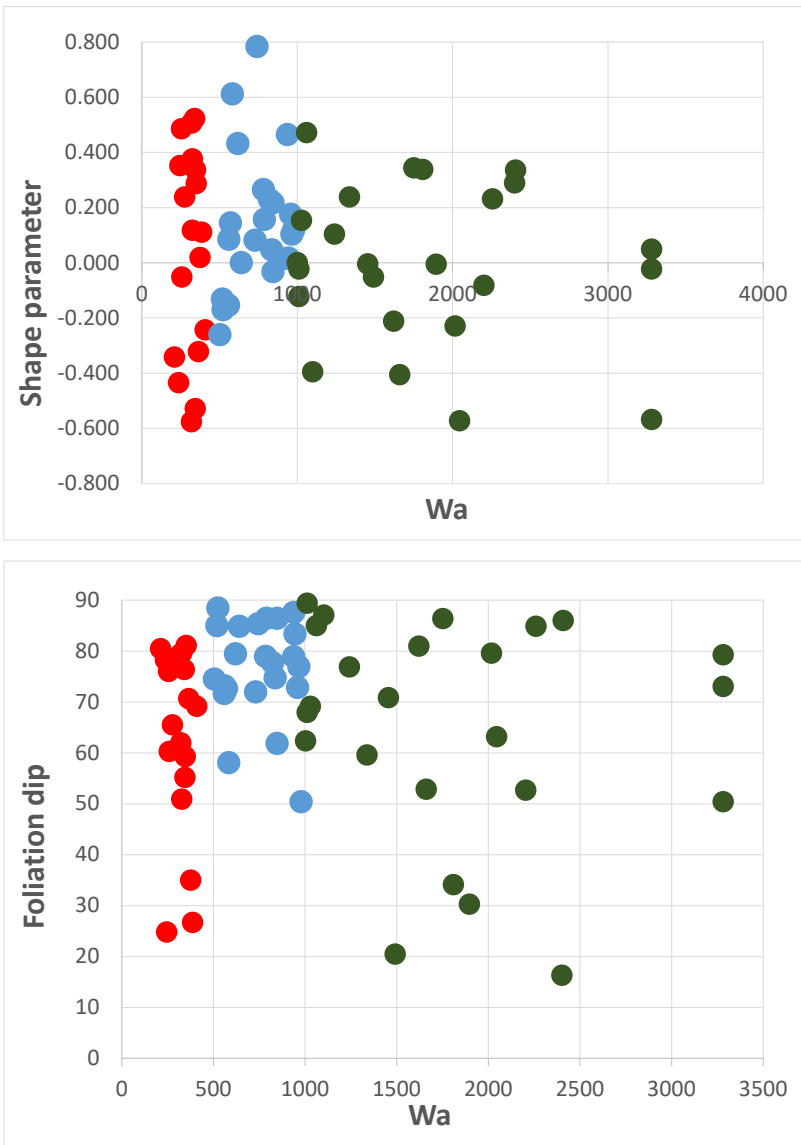
Frequency-susceptibility dependence

Diagram explanation  
X(1,4) X(4,16) X(1,16)



## DATA REPOSITORY ITEM 9

Station	Ds	Wa	Error	Kb	P	St deviat T	St dev	Lin plunge	Fol dip	
FT153	47	210	40	4.71E-03	1.008	0.001	-0.341	0.132	45	81
FT107	127	236	40	2.70E-04	1.017	0.006	-0.434	0.134	40	78
FT150	104	244	40	6.71E-04	1.011	0.001	0.353	0.138	7	25
FT154	-5	254	40	3.83E-03	1.038	0.002	0.486	0.082	29	76
FT152	118	257	40	1.95E-03	1.031	0.002	-0.051	0.145	47	60
FT159	103	275	40	1.60E-04	1.007	0.001	0.239	0.072	8	66
FT108	-54	318	40	9.72E-04	1.055	0.007	-0.576	0.063	48	79
FT113	-105	321	40	1.16E-03	1.026	0.003	0.507	0.078	22	62
FT151	96	325	40	3.80E-03	1.011	0.001	0.377	0.173	45	80
FT114	133	325	40	1.99E-03	1.039	0.002	0.118	0.173	48	51
FT112	109	340	40	2.78E-03	1.034	0.003	0.523	0.071	31	76
FT110	121	343	40	1.06E-03	1.026	0.002	-0.528	0.082	42	55
FT109A	111	345	40	2.28E-03	1.014	0.003	0.338	0.105	49	59
FT115	173	350	40	1.72E-04	1.012	0.002	0.288	0.119	36	81
FT109B	-117	364	40	2.55E-03	1.019	0.002	-0.321	0.157	22	71
FT109C	-30	375	40	5.32E-03	1.020	0.002	0.020	0.175	31	35
FT111	105	385	40	3.35E-03	1.011	0.002	0.111	0.133	26	27
FT122	36	407	40	8.48E-03	1.027	0.002	-0.242	0.102	69	69
FT116	-112	503	40	3.16E-03	1.035	0.002	-0.260	0.081	17	75
FT100	242	518	40	2.05E-03	1.021	0.001	-0.131	0.040	76	85
FT121	112	522	40	1.61E-04	1.011	0.007	-0.169	0.223	64	89
FT098	-105	557	40	4.61E-03	1.028	0.001	-0.153	0.124	18	72
FT120	50	560	40	4.45E-03	1.018	0.001	0.086	0.110	70	73
FT063	-109	570	40	4.08E-05	1.018	0.007	0.145	0.168	11	73
FT117	-85	582	40	6.18E-04	1.016	0.001	0.613	0.122	46	58
FT013	-128	618	40	3.95E-03	1.043	0.003	0.433	0.085	70	80
FT099	231	640	40	4.20E-03	1.038	0.002	0.001	0.064	43	85
FT119	91	729	40	1.80E-04	1.008	0.001	0.083	0.146	54	72
FT118	64	742	40	9.17E-04	1.043	0.003	0.785	0.057	26	85
FT125	64	783	40	3.12E-03	1.048	0.002	0.266	0.062	33	79
FT014	-27	788	40	2.75E-04	1.018	0.005	0.158	0.196	55	87
FT068	388	822	40	5.56E-04	1.009	0.002	0.230	0.224	66	78
FT066	-271	835	40	1.06E-02	1.027	0.002	0.048	0.145	66	75
FT161	243	845	40	4.88E-03	1.016	0.002	0.218	0.177	63	87



FT160	339	845	40	5.69E-03	1.032	0.003	-0.031	0.067	7	62
FT123	67	936	40	4.33E-03	1.044	0.002	0.466	0.077	25	79
FT126	104	936	40	1.67E-04	1.007	0.002	0.016	0.227	13	88
FT124	216	944	40	2.15E-04	1.006	0.002	0.018	0.225	17	83
FT102	147	958	40	2.37E-04	1.023	0.004	0.176	0.252	67	73
FT103	-447	965	40	1.85E-04	1.010	0.003	0.104	0.146	59	77
FT104	273	977	40	2.44E-04	1.007	0.002	0.121	0.172	28	50
FT158	79	1001	40	4.06E-03	1.010	0.002	0.001	0.171	11	62
FT141	-160	1010	40	3.13E-03	1.024	0.002	-0.022	0.110	88	89
FT138	276	1010	40	2.52E-03	1.033	0.003	-0.122	0.123	68	68
FT140	70	1027	40	1.61E-04	1.005	0.001	0.154	0.105	7	69
FT139	93	1060	40	1.26E-02	1.019	0.002	0.472	0.133	75	85
FT127	19	1100	40	2.26E-03	1.021	0.002	-0.394	0.159	9	87
FT143	-72	1240	40	2.36E-04	1.012	0.002	0.105	0.143	12	77
FT149	165	1337	40	1.60E-04	1.014	0.003	0.239	0.121	40	60
FT142	-585	1453	40	2.03E-04	1.007	0.001	-0.003	0.215	67	71
FT135	-707	1490	40	1.56E-04	1.011	0.003	-0.051	0.262	14	21
FT136	-600	1620	40	2.32E-04	1.019	0.003	-0.211	0.093	28	81
FT130	-334	1660	40	1.18E-04	1.008	0.012	-0.405	0.167	36	53
FT147	221	1750	40	4.92E-03	1.031	0.003	0.345	0.126	82	86
FT131	-62	1807	40	2.11E-04	1.016	0.003	0.339	0.129	32	34
FT133	15	1895	40	1.96E-04	1.009	0.001	-0.004	0.044	6	30
FT132	30	2016	40	1.10E-04	1.007	0.001	-0.229	0.129	11	80
FT137	93	2044	40	4.41E-03	1.031	0.002	-0.572	0.057	41	63
FT155	-404	2202	40	2.00E-04	1.009	0.002	-0.081	0.169	21	53
FT134	272	2258	40	2.22E-03	1.021	0.002	0.232	0.087	71	85
FT129	965	2400	40	1.80E-04	1.014	0.002	0.290	0.137	6	16
FT128	862	2406	40	1.23E-04	1.009	0.001	0.337	0.111	14	86
FT144	-785	3280	40	2.59E-04	1.009	0.002	-0.022	0.202	8	79
FT146	-208	3280	40	4.81E-03	1.031	0.002	-0.567	0.113	39	50
FT148	1432	3280	40	2.06E-03	1.008	0.001	0.050	0.208	73	73

